Available online at www.sciencedirect.com

ScienceDirect

Procedia CIRP 93 (2020) 1411–1416

www.elsevier.com/locate/procedia

53rd CIRP Conference on Manufacturing Systems

# Tool and Workpiece Deflection Induced Flatness Errors in Milling of Thin-walled Components

Ankit Agarwal, K. A. Desai*

*Department of Mechanical Engineering, Indian Institute of Technology Jodhpur, Jodhpur-342037, Rajasthan, India*

**Abstract**

The static deflections of cutting tool and thin-walled components during end milling operation contribute significantly towards deviation of a machined surface from the desired level resulting in violation of tolerances. The designer specifies tolerances as per Geometric Dimensioning and Tolerancing (GD&T) standard (ASME Y14.5-2009 or ISO 1101) to transfer designer intent to the manufacturer. The machined surface deviation for straight components translates into flatness error, defined as the normal distance between the two parallel planes encompassing distorted points. This paper investigates the relative contributions of tool and workpiece deflections on the flatness error during end milling of thin-walled components. It is attempted by developing computational models to estimate cutting forces, tool-workpiece deflections and flatness error with associated parameters. A set of end milling experiments are conducted on thin-walled components to substantiate the results.It has been observed that the contribution of tool and workpiece deflections on flatness error has significant dependence on the cutting widths. The outcomes of the present study provides meaningful insights to the manufacturing process planners in determining optimal cutting conditions and strategies to control flatness error during machining of thin-walled components.



*Keywords:* Flatness; End Milling; Thin-walled components; Tool Deflections; Workpiece Deflections

## 1. Introduction

End milling operation is commonly employed to fabricate thin-walled components as it can produce intricate shapes with superior quality and higher productivity. In spite of these advantages, the application of end milling is restricted due to process faults such as the static deflections of cutting tool and workpiece, fixturing errors, cutter runout, tool wear, vibrations etc. The static deflections of an end mill and workpiece (for thin-walled components) are major causes of violating tolerance specifications envisaged by the designer. Geometric Dimensioning and Tolerancing (GD&T) principles defined by ASME Y14.5-2009 [1], or ISO 1101 [2] standards are employed in recent times to communicate tolerance specifications to the manufacturer. GD&T offers several benefits to the designer and manufacturing personnel by minimizing the guesswork and assuring the transfer of appropriate information across various stages of product development. GD&T principles estimate the variation of machined components from the intended design in terms of straightness/flatness error for 2D/3D planar components. The flatness error of a component is designated using two attributes, (i) perpendicular distance between two parallel planes encompassing point-cloud representing machined surface and, (ii) inclination of the normal to the parallel planes. As end mill and thin-walled component are considerably flexible, both are prone to deflections under the action of periodically varying cutting forces during milling operation.

The end milling of thin-walled components has been extensively studied and reported in the literature. The studies can be categorized into the following; modeling of cutting forces, estimation of machining attributes such as tool-workpiece deflections, surface error, etc. and control of machining errors. The Mechanistic force model correlates cutting forces with the uncut chip area using empirical constants [3] and it is employed commonly for milling operation. The model evolved over the years by introducing the influence of process attributes such as cutter runout [4], size effect [5], tool and workpiece deflections

* Corresponding author. Tel.: +91-291 280 1509;
*E-mail address:* kadesai@iitj.ac.in (K. A. Desai).

2212-8271 
10.1016/j.procir.2020.04.101

[6], etc. The models for estimation and control of deflection induced surface errors for thin-walled components are also reported in the literature. The variation of surface error during milling of thin-walled plates was studied considering tool and workpiece deflections [7]. The Finite Element Analysis (FEA) based approach was suggested to predict [8] and compensate [9] static deflection induced surface errors during machining of thin-walled components. Dépincé and Hascoët [10] estimated tool deflections and proposed tool path compensation technique to minimize errors. The classification scheme for the axial profile of surface error was conceived in the presence of static deflections of cutting tool [11] and thin-walled workpieces [12]. The FEA based methodology is explored to highlight the effect of workpiece thickness [13], process parameters and cutting temperature [14] on workpiece deflections during end milling of thin-walled components. The prediction of form error during 5-axis milling of thin-walled components is attempted recently [15]. Obeidat and Raman [16] optimized the requirement of inspection points to determine the flatness error by determining the location of maximum workpiece deflection. Mikó and Rácz [17] examined the influence of surface roughness on flatness and angularity error during the ball-end milling operation and concluded that the assessment of surface error is entirely different from flatness values.

Based on the review of literature, it has been realized that the estimation and control of dimensional error due to tool-workpiece deflections is investigated thoroughly. There has been no study that analyzes flatness error due to the static deflections of tool and workpiece during end milling of thin-walled components. The studies do not quantify the independent contribution of tool and workpiece deflections on flatness error over a wide range of cutting widths. It has been reported in the literature that the nature and magnitude of cutting tool [11] and workpiece [12] deflections differ from each other and it can be closely linked with cutting widths (*RDOC* and *ADOC*). This paper presents a methodology to predict flatness error and realizes the quantitative assessment of tool and workpiece deflection towards flatness error by performing computational studies and machining experiments over range of *ADOC*. The present methodology can be implemented in the form of computational tool that assist process planners in deciding the values of cutting parameters (*RDOC*, *ADOC*, Feed rate) clamping state of the workpiece and sequences of the material to be removed for limiting tolerances within the intent of the designer.

## 2. Modeling of Flatness Error

The prediction of flatness error during end milling of thin-walled components necessitates an integration of several computational models. It includes cutting force model, tool-workpiece deflection models and a mechanism to transform deflections into flatness error. The subsequent subsections summarize these models in estimating flatness error during end milling of thin-walled planar components.

### 2.1. Modeling of Cutting Forces

The Mechanistic force model has been adopted in this study to predict cutting forces during end milling of thin-walled components. The model predicts cutting forces by dividing an end mill into disk elements ($n$) of equal thickness ($dz$) along the axial direction. The model estimates Feed ($F_F$) and Normal ($F_N$) components of the cutting force for each engaged flute ($k$) at an incremental rotation of the cutter ($i$) for individual axial disk elements ($j$) using Eqs. 1-3. The total force $F_s^T(\phi_i)$ $(s = F, N)$ at a cutter rotation angle ($\phi_i$) can be obtained by integrating forces acting on individual disk elements for each engaged flute using Eq. 4.

In Eq. 1, $t_c(i, j, k)$ and $\beta(i, j, k)$ represent instantaneous uncut chip thickness and angular position corresponding to $j^{th}$ disk element and $k^{th}$ flute at cutter rotation angle $\phi_i$. The uncut chip thickness $t_c(i, j, k)$ can be expressed geometrically using Eq. 2 as a function of feed per tooth ($f_{pt}$). The angular position $\beta(i, j, k)$ can be determined using Eq. 3, where $\phi_p$, $\theta_h$, $R_c$ represents pitch angle, helix angle and radius of the cutter respectively.

$$\begin{bmatrix} F_F(i,j,k) \\ F_N(i,j,k) \end{bmatrix} = dz\ t_c(i,j,k) \begin{bmatrix} cos\,\beta(i,j,k) & -sin\,\beta(i,j,k) \\ sin\,\beta(i,j,k) & cos\,\beta(i,j,k) \end{bmatrix} \begin{bmatrix} K_T(i,j,k) \\ K_R(i,j,k) \end{bmatrix} \tag{1}$$

$$t_c(i,j,k) = f_{pt}\ sin\,\beta(i,j,k) \tag{2}$$

$$\beta(i,j,k) = \phi_i + (k-1)\,\phi_p + \left((j-1)\,dz + \frac{dz}{2}\right)\frac{tan\,(\theta_h)}{R_c} \tag{3}$$

$$F_s^T(\phi_i) = \sum_{i,j,k} F_s(i,j,k) \qquad s = F, N \tag{4}$$

$$K_q(i,j,k) = a_q\ e^{-b_q\ t_c(i,j,k)} + c_q \qquad (q = T, R) \tag{5}$$

The terms $K_q(i, j, k)$ $(q = T, R)$, in Eq. 1 are known as Mechanistic cutting constants, and it correlates instantaneous uncut chip thickness with cutting forces. These constants can be determined by performing end milling experiments under specific conditions for a given combination of tool and workpiece material. The non-linear relationship between cutting constant $K_q(i, j, k)$ $(q = T, R)$ and instantaneous uncut chip thickness $t_c(i, j, k)$ can be derived subsequently using curve fitting (Eq. 5).

### 2.2. Modeling of Distorted Surface

The thin-walled components are inherently flexible and prone to static deflections under the application of cutting forces during the end milling operation. Similarly, the end mill is another flexible element of the milling system that also deflects considerably under the action of periodically varying forces. The static deflections of tool and workpiece contribute significantly towards machined surface error and violation of

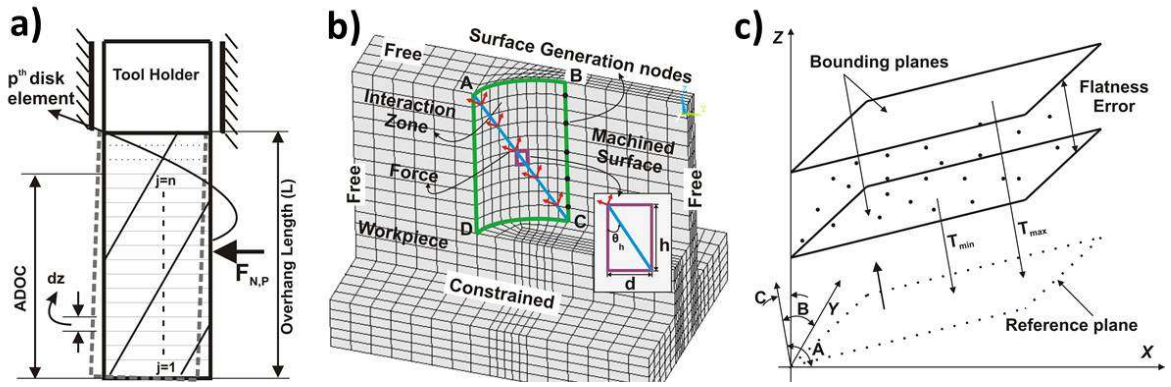


Fig. 1. Modeling of Flatness Error: (a) Tool Deflection; (b) Workpiece Deflection; (c) Flatness Error Estimation

geometric tolerances. This section presents computational models to estimate tool-workpiece deflections and mechanism to transform the same into flatness error parameters.

### 2.2.1. Tool Deflection

The present study considers end mill as a Cantilever beam with non-uniform forces acting in the cutter-workpiece interaction zone. The model uses the concept of equivalent diameter $D_e$ to incorporate the effect of cutting flutes on deflections of an end mill [18]. The tool deflection model enables the direct transfer of cutting forces from the Mechanistic force model by considering the identical thickness of axial disk elements ($dz$) in both models as depicted in Fig. 1(a). The cantilever beam formulation estimates static deflection of an individual disk element ($j$) in the normal direction due to cutting forces acting on each $p^{th}$ engaged elements.

### 2.2.2. Workpiece Deflection

The cutting force data estimated using the Mechanistic model are input to 3-Dimensional (3-D) FEA model to estimate static deflections of thin-walled components. The component has been modeled by employing ANSYS Parametric Design Language (APDL) environment and meshed using a 3-D 8-node solid shell element (SOLSH 190). The thin-walled component is fixed in the FEA model such that it is free to deflect along three sides (top, left, right) and constrained from the bottom, as depicted in Fig. 1(b). The tool-workpiece interaction zone at a given instant is marked as ABCD and cutting forces are transferred to this zone as presented in Fig. 1(b). The height ($h$) of the quad element in the FEA model is kept identical to the thickness of the disk element ($dz$) in the Mechanistic model to facilitate direct transfer of force components. The cutting forces are applied along a slant line (AC) to depict the helical edge of the cutting flute. The flute generates the machined surface gradually while leaving the cut along the line CB. The deflections of nodes lying on the edge CB of the interaction zone are recorded for the estimation of deflected coordinates representing the machined surface. These steps are to be repeated at each incremental rotation of the cutter until the flute traverses the interaction zone completely. It is required to estimate static deflections of the component at different locations ($L = 10\%, 20\%, ....., 90\%$) along the feed direction to appreciate the effect of rigidity variation [6].

### 2.2.3. Estimation of Distorted Coordinates

Once static deflections of end mill and thin-walled components are estimated, the data is transformed in the form of distorted point cloud representing machined surface to estimate flatness error. The distorted points are obtained by subtracting deflection value $def_c(L, j)$ computed for $j^{th}$ disk element on the exit edge CB at $L^{th}$ location along the feed direction from Cartesian coordinates $acor_c(L, j)$ of the corresponding nodal point. Eq. 6 shows the mathematical formulation to determine deflected coordinates $dcor_c(L, j)$ at a given axial location.

$$dcor_c(L, j) = acor_c(L, j) - def_c(L, j) \qquad (c = x, y, z) \qquad (6)$$

### 2.3. Estimation of Flatness Error

The flatness error is defined as the orthogonal distance between two parallel planes encompassing distorted coordinates $dcor_c(L, j)$ representing the machined surface, as depicted in Fig. 1(c). The present study employs Particle Swarm Optimization (PSO) algorithm [19] for estimation of the flatness error [20, 21]. The distorted coordinates $dcor_c(L, j)$ obtained in Section 2.2 are input to the PSO algorithm and flatness error is determined by minimizing the objective function given using Eq.7. The objective function depends on parameters ($P$) related to a planar surface from which the minimum normal distance between the nearest and farthest points are optimized. The planar surface is represented using Eq. 8 where, $cos(Q)$ ($Q = A, B, C$) represents direction cosines of a normal to the reference plane while $D$ is constant representing intercept along $Z$-axis.

$$Min\,[F(P) = Max\,(T_t) - Min\,(T_t)] \qquad (P = A, B, C, D) \qquad (7)$$

$$T_t = dcor_x\,cos(A) + dcor_y\,cos(B) + dcor_z\,cos(C) - D \qquad (8)$$

Figure 2 shows an overall computational framework proposed in this study to determine flatness error during end milling of thin-walled components. The methodology can be

Table 1. Computational and Experimental Flatness Values.

| Test No. | RDOC (mm) | ADOC (mm) | Computational (mm) Workpiece | Computational (mm) Tool-workpiece | Experimental (mm) | Relative Contribution (%) Tool | Relative Contribution (%) Workpiece | Remarks |
|---|---|---|---|---|---|---|---|---|
| 1. | 4 | 4 | 8.563 | 26.428 | 32.919 | 67.60 | 32.4 | Tool Dominant |
| 2. | | 11 | 58.224 | 68.686 | 67.259 | 15.24 | 84.76 | |
| 3. | | 18 | 77.433 | 83.553 | 85.056 | 7.33 | 92.67 | |
| 4. | | 25 | 149.394 | 157.830 | 161.519 | 5.34 | 94.65 | W/p Dominant |

| Cutting Parameters | | | Tool Attributes (Kennametal - Solid Carbide) | | | Workpiece Attributes (Aluminium 6061-T6) | | |
|---|---|---|---|---|---|---|---|---|
| Feed (mm/min) | : | 300 | Cutter Diameter (mm) | : | 16 | Young's Modulus | : | 68.9 GPA |
| Spindle Speed (RPM) | : | 2000 | Helix Angle | : | 30° | Poisson's Ratio | : | 0.33 |
| | | | No. of Flutes | : | 4 | Dimension (L x H x D) | : | 100 x 50 x 6 |

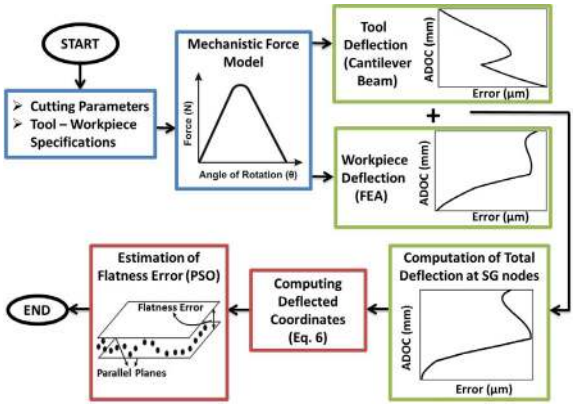


Fig. 2. Methodology for estimation of flatness error

divided into three stages broadly; the first stage consists of integrating the Mechanistic force model with the tool and workpiece deflection models. The second stage deals with the estimation of tool-workpiece deflections. The third stage deals with the transformation of deflection data into the flatness error. An automated program is developed in this study to compute flatness error along with associated parameters during milling of thin-walled components.

## 3. Results and Discussion

A set of computational models outlined in the previous section are employed to determine flatness errors and estimate relative contribution of tool and workpiece deflections during end milling of thin-walled components. The flatness error is estimated using two approaches; the first approach neglects tool deflections while the second approach uses both tool and workpiece deflections in predicting flatness error. The difference of flatness value between both approaches reflects the contribution of tool deflections towards the error. Section 3.1 presents cutting conditions where tool deflections dominate the flatness error as the rigidity of the thin-walled component is comparatively higher. Section 3.2 presents machining of the substantially thin-walled component where both tool and workpiece deflections contribute towards the flatness error. Section 3.3 summarizes machining of thin-walled components at elevated cutting conditions where workpiece deflections dominate the flatness error. Table 1 summarizes the cutting conditions used for the above cases, workpiece material along with relevant properties, and cutting tool specifications. The machining experiments were conducted on a 3-axis CNC vertical milling machine and measurement experiments were performed using a spindle mounted inspection probe (Renishaw OMP-400) as depicted in Fig. 3.

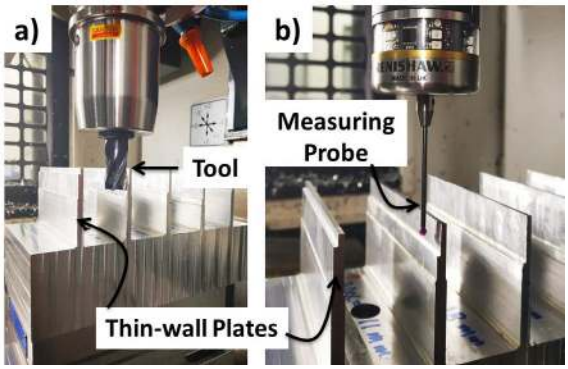


Fig. 3. Experimental Setup: a) Machining Setup; b) Measurement Setup

### 3.1. Tool Deflection Dominant Conditions

Figure 4 shows flatness error estimated computationally and measured experimentally for cutting conditions corresponding to Test 1 (Table 1). The objective of this case is to examine the relative contribution of tool and workpiece deflections on flatness error during machining of thin-walled components at lower Axial Depths of Cut (*ADOC*). It can be seen that the flatness error estimated from workpiece deflection model (Fig. 4(a)) is very small in comparison to the value estimated by combining both tool and workpiece deflections (Fig. 4(b)). Although the end mill experiences comparatively smaller force at lower *ADOC*, it accords for almost 70% of the flatness error. The lower workpiece deflections are attributed to higher rigidity of the thin-walled components and less material being removed at lower *ADOC*. The contribution of tool deflections is significant at lower *ADOC* and it must be incorporated in the

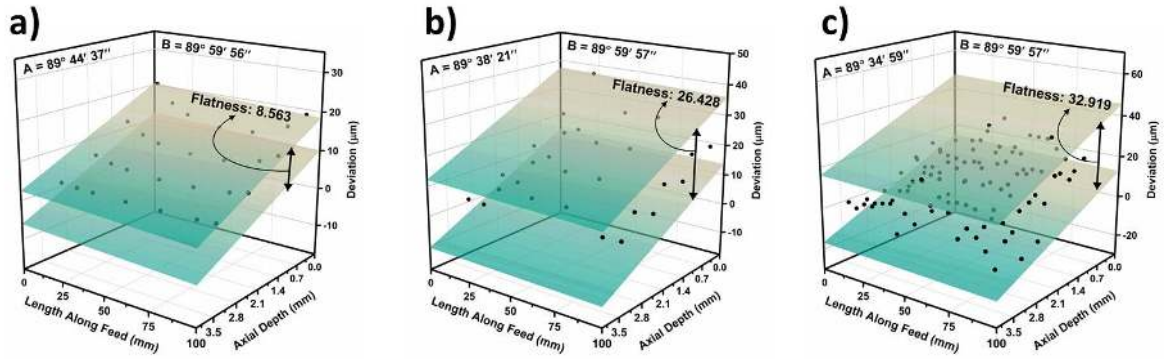


Fig. 4. Flatness Error (Test 1): a) Workpiece Deflection (Computational); b) Tool-Workpiece Deflection (Computational); c) Experimental Results

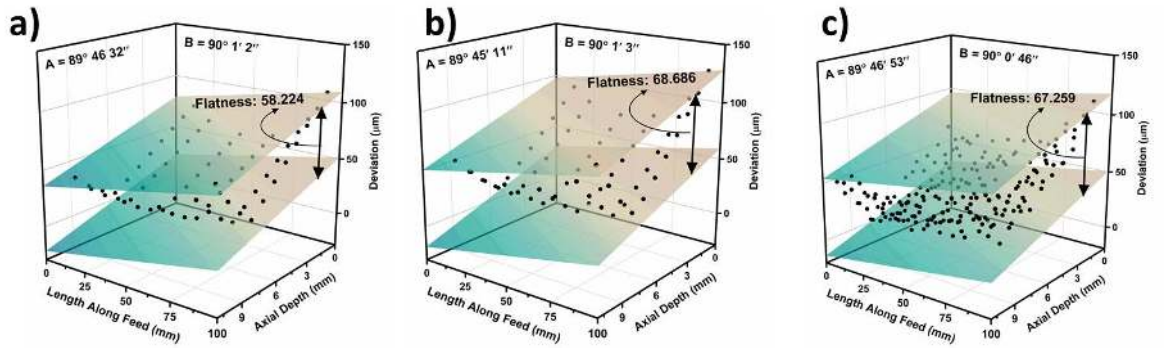


Fig. 5. Flatness Error (Test 2): a) Workpiece Deflection (Computational); b) Tool-Workpiece Deflection (Computational); c) Experimental Results

computational models estimating flatness error for better prediction accuracy.

### 3.2. Tool-Workpiece Deflection Dominant Conditions

The study considers tests 2 and 3 (Table 1) to investigate the effect of tool and workpiece deflections on flatness error with increasing Axial Depths of Cut (*ADOC*). Figure 5 shows flatness error determined computationally and measured experimentally for cutting conditions corresponding to Test 2. The results showed that the contribution of tool deflection towards flatness error is reduced significantly at higher *ADOC* (about 10-20% of the flatness error). As *ADOC* increases, the amount of material being removed during the cut also increases in comparison to the previous case (Section 3.1). The increase of material removal during the cut reduces the rigidity of the component with the progress of operation and increased workpiece deflections. It can be inferred that the contribution of both tool and workpiece deflections on flatness error is significant at elevated cutting conditions (similar to roughing operation) during end milling of thin-walled components.

### 3.3. Workpiece Deflection Dominant Condition

Figure 6 shows flatness error obtained computationally and measured experimentally for cutting conditions corresponding to Test 4 (Table 1). The objective of these tests is to examine the relative contribution of tool and workpiece deflections towards flatness error during machining thin-walled components at very high Axial Depth of Cut (*ADOC*) which is representative of large material being removed during the cut. It can be seen that flatness error from the workpiece deflection model (Fig. 6(a)) is identical to the values computed using the combined tool and workpiece deflections (Fig. 6(b)). It is expected commonly that the tool deflection will be significant at higher *ADOC* and contributes majorly towards flatness error. The results show that the tool deflection contributes only 5% to the total flatness error. As the rigidity of the thin-walled component is reduced remarkably due to a large amount of material being removed at higher *ADOC*, workpiece deflections increase considerably in comparison to tool deflections. Although the magnitude of tool deflections is higher, its contribution to the total flatness error is relatively small as seen from computational and experimental results presented in Fig. 6. The increased contribution of workpiece deflections can be attributed to considerable thinning of the component with the progress of milling operation. The increased thinning of the component with progress of machining results into widening of the distorted point cloud from start to end of the cut as seen in Fig. 6. The wider error profile is reflected in the form of higher flatness error for these conditions. Based on the outcomes of the present study, it has been observed that the static deflections of tool and workpiece both contribute to the flatness error under different cutting conditions. It is necessary to incorporate both these models in the

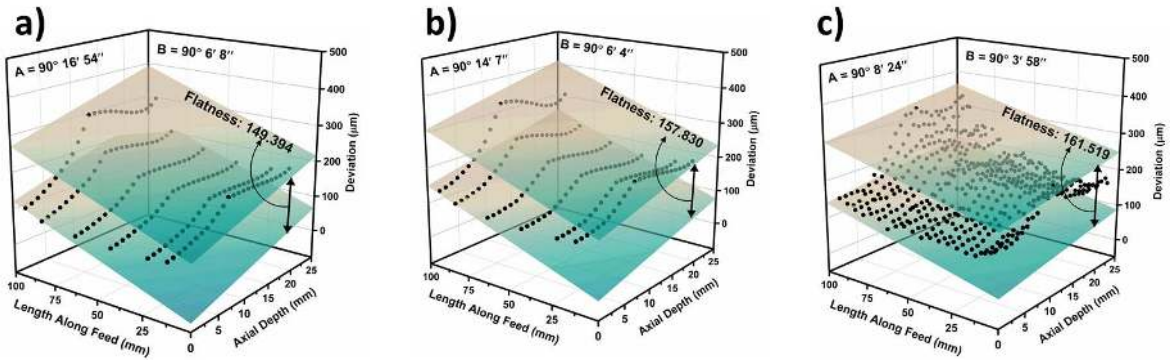


Fig. 6. Flatness Error (Test 4): a) Workpiece Deflection (Computational); b) Tool-Workpiece Deflection (Computational); c) Experimental Results

computational framework for improved prediction accuracy of the flatness estimation model.

## 4. Conclusions

This paper presents an overall framework to estimate and analyze the relative contribution of tool-workpiece deflections on the flatness error during end milling of thin-walled components. The study uses two different computational approaches to substantiate this aspect and the outcomes are validated by conducting machining experiments. Based on results presented in the study, it is realized that the static deflections of the end mill contribute significantly to the flatness error at lower *ADOC* values. The same can be attributed to the higher rigidity of thin-walled components at these cutting conditions thereby reduced contribution from workpiece deflections. The study also investigated the effect of an increase of *ADOC* and its effects on tool deflections and resultant flatness error. It was observed that the contribution of tool deflections to flatness error reduces considerably at higher *ADOC*. The observations at higher *ADOC* are in contrast to the general comprehension which expects higher contribution to the flatness error. The outcomes of the present study provide meaningful information to the process planners and assists in the selection of appropriate cutting conditions, tool-path planning, developing fixturing strategies/support systems, etc. during end milling of thin-walled components.

## Acknowledgements

The authors thank DST - Science and Engineering Research Board (SERB) (Project No.: YSS/2015/000495) and Ministry of Human Resource Development (MHRD), India for providing financial support to carry out this research work.

## References

[1] ASME Y14.5-2009 Geometric Dimensioning and Tolerancing- Application, Analysis & Measurement, ASME Press.
[2] ISO 1101:2017 Geometrical Product Specifications (GPS)-Geometrical Tolerancing-Tolerances of Form, Orientation, Location and Run-Out, Geneva, Switzerland.
[3] Sabberwal, A. J. P., Koenigsberger, F., 1961. Chip section and cutting force during the milling operation. CIRP Ann, 10(3), 197-203.
[4] Sutherland, J. W., Devor, R., 1986. An improved method for cutting force and surface error prediction in flexible end milling systems. J Eng Ind, 108(4), 269-279.
[5] Ko, J. H., Yun, W. S., Cho, D. W., Ehmann, K. F., 2002. Development of a virtual machining system, part 1: approximation of the size effect for cutting force prediction. Int J Mach Tools Manuf, 42(15), 1595-1605.
[6] Wan, M., Zhang, W. H., 2006. Calculations of chip thickness and cutting forces in flexible end milling. Int J Adv Manuf Technol, 29(7-8), 637-647.
[7] Budak, E., Altintas, Y., 1995. Modeling and avoidance of static form errors in peripheral milling of plates. Int J Mach Tools Manuf, 35(3), 459-476.
[8] Wan, M., Zhang, W., Qiu, K., Gao, T., Yang, Y., 2005. Numerical prediction of static form errors in peripheral milling of thin-walled workpieces with irregular meshes. J Manuf Sci Eng, 127(1), 13-22.
[9] Ratchev, S., Liu, S., Huang, W., Becker, A. A., 2004. Milling error prediction and compensation in machining of low-rigidity parts. Int J Mach Tools Manuf, 44(15), 1629-1641.
[10] Dépincé, P., Hascoët, J.Y., 2006. Active integration of tool deflection effects in end milling. Part 2. Compensation of tool deflection. Int J Mach Tools Manuf, 46(9), 945-956.
[11] Desai, K. A., Rao, P. V. M., 2012. On cutter deflection surface errors in peripheral milling. J Mater Process Technol, 212(11),2443-2454.
[12] Arora, N., Agarwal, A., Desai, K. A., 2019. Modelling of static surface error in end-milling of thin-walled geometries. Int J Precis Technol, 8(2-4),107-123.
[13] Wang, J., Ibaraki, S., Matsubara, A., Shida, K., Yamada, T., 2015. FEM-based simulation for workpiece deformation in thin-wall milling. Int J Autom Technol, 9(2), 122-128.
[14] Bolar, G., Joshi, S. N., 2017. Three-dimensional numerical modeling, simulation and experimental validation of milling of a thin-wall component. Proc Inst Mech Eng, Part B: J Eng Manuf, 231(5), 792-804.
[15] Li, Z.L., Tuysuz, O., Zhu, L.M., Altintas, Y., 2018. Surface form error prediction in five-axis flank milling of thin-walled parts. Int. J. Mach. Tools Manuf. 128, 21-32.
[16] Obeidat S. M., Raman S., 2011. Process-guided coordinate sampling of end-milled flat plates. Int J Adv Manuf Technol, 53(9-12), 979-991.
[17] Mikó B., Rácz G., 2018. Investigation of Flatness and Angularity in Case of Ball-End Milling. Int Symp Prod Res, 65-72, Springer, Cham.
[18] Kops, L., Vo, D. T., 1990. Determination of the equivalent diameter of an end mill based on its compliance. CIRP Ann, 39(1), 93-96.
[19] Eberhart R., Kennedy J., 1995. A new optimizer using particle swarm theory. InMHS'95. Proc Sixth Int Symp Micro Mach Hum Sci, IEEE, 39-43.
[20] Kovvur Y., Ramaswami H., Anand R. B., Anand S., (2008). Minimum-zone form tolerance evaluation using particle swarm optimisation. Int J Intell Syst Technol Appl, 4(1-2), 79-96.
[21] Pathak V. K., Singh A. K., Singh R., Chaudhary H., 2017. A modified algorithm of Particle Swarm Optimization for form error evaluation. tm - Tech Mess, 84(4), 272-292.